

# In situ structural and texture analyses of monoclinic phase for polycrystalline Ni-rich Ti<sub>49.86</sub>Ni<sub>50.14</sub> alloy from neutron diffraction data

Husin Sitepu

Crystallography Laboratory, Virginia Tech, Blacksburg, Virginia 24061, USA and Department of Physics, College of Science, Sultan Qaboos University, P.O. Box 36, Postal Code 123, Muscat, Oman

(Received 10 December 2007; accepted 11 January 2008)

Phase transformation temperatures of a polycrystalline Ni-rich Ti<sub>49.86</sub>Ni<sub>50.14</sub> shape memory alloy were investigated using a differential scanning calorimeter. *In situ* structural and texture analyses of the monoclinic Ti<sub>49.86</sub>Ni<sub>50.14</sub> were investigated using neutron powder diffractometer technique. Differential scanning calorimeter results showed that this Ni-rich alloy has a one-step cubic to monoclinic martensitic phase transformation on cooling and a one-step monoclinic to cubic transformation on heating. *In situ* high-resolution neutron powder diffraction data of the monoclinic phase from low temperatures to room temperature on heating are consistent with the differential scanning calorimeter's heating results. In addition, the refined monoclinic crystal structure parameters for all neutron diffraction data sets agree satisfactorily with single-crystal X-ray diffraction results. The multiple-data-set capabilities of the GSAS Rietveld refinement program, with a generalized spherical-harmonics description was used successfully to extract the texture description directly from a simultaneous refinement using 52 time-of-flight monoclinic neutron diffraction patterns, taken from a polycrystalline sample held in 13 orientations inside the diffractometer. © 2008 International Centre for Diffraction Data. [DOI: 10.1154/1.2839141]

Key words: neutron powder diffraction, texture, martensitic phase transformation, Ti<sub>49.86</sub>Ni<sub>50.14</sub> shape memory alloy, differential scanning calorimeter

## I. INTRODUCTION

Technologically important polycrystalline Ti-Ni shape memory alloy undergoes one-stage martensitic phase transformation from cubic (austenite, *B2* phase) at the high temperatures to monoclinic (martensitic, *B19* phase) at low temperatures, and one-step monoclinic to cubic transformation on heating [see Otsuka and Ren (2005), Sitepu (2007), and references therein]. A high-temperature single-crystal X-ray diffraction study reported by Wang *et al.* (1965) revealed a cubic phase at above the martensitic transformation starting temperature for the Ti<sub>50</sub>Ni<sub>50</sub> binary alloy with  $a=3.01$  Å, space group *Pm3m* (No. 221), and  $Z=1$ , with Ni atoms occupying the  $1a$  (0, 0, 0) Wyckoff positions and Ti atoms occupying the  $1b$  (0.5, 0.5, 0.5) positions. Crystal structure of the monoclinic phase of the Ti<sub>50.80</sub>Ni<sub>49.20</sub> alloy was successfully determined using a single-crystal X-ray diffraction technique (Kudoh *et al.*, 1985). The initial monoclinic structure parameters of the single-crystal electron diffraction pattern of Ti<sub>50</sub>Ni<sub>50</sub> alloy reported originally by Michal and Sinclair (1981) were used, and Kudoh *et al.* (1985) reported that the space group is *P112<sub>1</sub>/m* and  $Z=2$ , which agrees quite satisfactorily with those results reported by Michal and Sinclair (1981). The quality of the single-crystal X-ray diffraction data with 377 observed reflections investigated by Kudoh *et al.* (1985) was superior to those single-crystal electron diffraction data with 22 observed reflections obtained by Michal and Sinclair (1981), and atomic parameters and temperature factors were successfully refined and yielded the crystallographic  $R_p$ -factor of 4.5%, which is smaller than that of results reported by Michal and Sinclair (1981).

Because it is quite difficult to grow sufficiently large single crystals of the monoclinic phase of the Ti-Ni shape memory alloys and produce martensite from TiNi powder,

polycrystalline samples were used. It is possible to extract texture (or preferred orientation) information from powder diffraction data of a polycrystalline alloys if the pattern for a randomly oriented specimen can be modeled (or simulated) from crystal structure parameters and other related factors such as line broadening resulting from size and strain parameters (Sitepu, 2002; Sitepu, 2003; Sitepu *et al.*, 2005). The pertinent attribute of neutrons with respect to structural refinement and texture analysis is the small absorption coefficients of neutrons for most materials, compared to those of X-rays. Therefore, neutron crystal structure and texture information are from the bulk of the sample, whereas those for X-rays are typically from near the surface. Additionally, the strong contrast between neutron scattering lengths of Ti ( $-3.44 \times 10^{-15}$  m) and Ni ( $10.30 \times 10^{-15}$  m) allows site occupancies of these two atoms to be refined with far greater reliability than can be achieved with X-ray diffraction (Sitepu, 2007).

In this paper, a differential scanning calorimeter technique was used to investigate the phase transformation temperatures of the polycrystalline Ni-rich Ti<sub>49.86</sub>Ni<sub>50.14</sub> shape memory alloy prepared from annealed solution at 850 °C for 15 min. Neutron diffraction technique was used to study *in situ* structure and texture analyses of the monoclinic phase of the alloy.

## II. EXPERIMENTAL

### A. Material and differential scanning calorimeter analysis

A cylindrical polycrystalline Ni-rich Ti<sub>49.86</sub>Ni<sub>50.14</sub> alloy with a diameter of 0.8 cm and 8 cm in height was machined from the as-received alloy rod. To make sure that the alloy

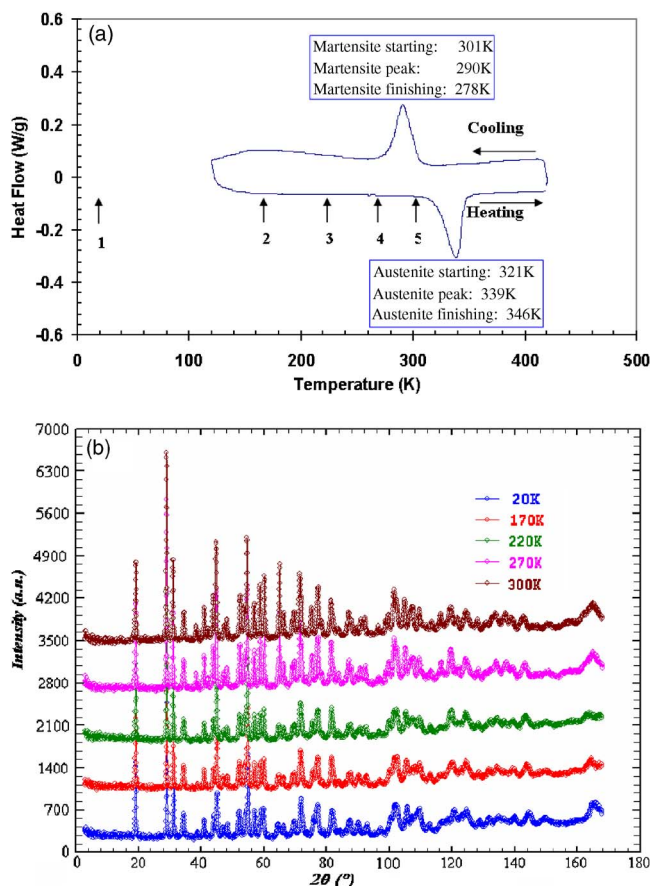


Figure 1. (Color online) (a) Differential scanning calorimeter curve of the Ni-rich  $\text{Ti}_{49.86}\text{Ni}_{50.14}$  shape memory alloy. The alloy with mass of 0.05 g was taken out from the annealed-solution material and then measured using a TA Instrument 2920 CE. The alloy was heated up to 373 K and started the differential scanning calorimeter measurement by cooling down to 173 K using a cooling rate of 10 K/min, and heating up from 173 to 373 K. (b) *In situ* high-resolution neutron powder diffraction patterns of monoclinic state in Ni-rich  $\text{Ti}_{49.86}\text{Ni}_{50.14}$  alloy measured at 20, 170, 220, 270, and 300 K on heating.

was homogeneous, this alloy was annealed at 1123 K for 15 min and then quenched in water (Sitepu *et al.*, 2002a). The differential scanning calorimeter results reveal one-step cubic to monoclinic martensitic transformation on cooling and one-step monoclinic to cubic transformation on heating [see Figure 1(a)]. The figure shows that the start and finish phase transformation temperatures are 301 and 278 K, respectively, for the monoclinic structure on cooling and 321 and 346 K, respectively, for the cubic phase on heating. Additionally, the peaks on the differential scanning calorimeter curve are at 290 K on cooling and 339 K on heating. Therefore, the thermal hysteresis loop of the monoclinic (martensitic,  $B19$ ) phase is centered approximately at room temperature. When the differential scanning calorimeter measurements were repeated, no change in the appearance of the transformation temperatures was detected.

### B. *In situ* high-resolution fixed-wavelength neutron powder diffraction data measurements

Neutron diffraction data of the monoclinic phase for the Ni-rich  $\text{Ti}_{49.86}\text{Ni}_{50.14}$  shape memory alloy were measured at 20, 170, 220, 270, and 300 K using the BT-1 high-resolution

fixed-wavelength 32-detector powder diffractometer at the National Institute of Standards and Technology (NIST) Center for Neutron Research in Gaithersburg, Maryland. The cylindrical shape of this alloy, 0.8 cm in diameter and 8 cm in height, corresponds to the dimensions of the primary neutron beam, which was chosen using an appropriate collimation. During our neutron diffraction data collection, the BT-1 instrument was equipped with a cryofurnace to heat and cool the alloy (with a temperature constant zone exceeding the length of the rod alloy). A Cu(311) monochromator with a  $90^\circ$  take-off angle and  $1.5402(1)$  Å wavelength was used. The scan range was  $10^\circ$  (i.e., two adjacent detectors with  $5^\circ$  scan range for each detector) with a step size of  $0.05^\circ$  so that each data point was collected in two adjacent detectors with a total scan range from  $3^\circ$  to  $168^\circ$ . After mounting the alloy in the cryofurnace, the alloy was slowly cooled down to 20 K. In each neutron diffraction measurement, the alloy was first heated up to each of the five selected temperatures (20, 170, 220, 270, and 300 K) and held at those temperatures for 6 min before neutron diffraction data were collected for 4 h. All data sets of the monoclinic phase collected at each temperature were then processed and combined to yield a single diffraction pattern using interpolations between adjacent observations to correct for zero-point offsets and detector sensitivities. Figure 1(b) shows that all neutron powder diffraction data sets of the monoclinic phase are consistent with the differential scanning calorimeter results on heating.

### C. *In situ* texture measurements using time-of-flight neutron diffractometer

The polycrystalline Ni-rich  $\text{Ti}_{49.86}\text{Ni}_{50.14}$  alloy was kept in liquid nitrogen for 15 min, so that the alloy was in the monoclinic state after they warmed up to 300 K. Time-of-flight neutron diffraction data of its monoclinic state were collected at this temperature on the high intensity powder diffractometer (HIPD) at the Los Alamos National Laboratory (LANSCE) in Los Alamos, New Mexico (Von Dreele, 1997; Sitepu *et al.*, 2002b). During a texture experiment, the HIPD was equipped with four detector banks at  $-153^\circ$ ,  $+153^\circ$ ,  $-90^\circ$ , and  $+90^\circ$  diffraction angles, and a two-axis ( $\Omega$  and  $\chi$ ) goniometer Eulerian angles ( $\Omega, \chi, \Phi$ ) to control the sample orientation was used. The  $\Omega$  circle of the goniometer Eulerian angle is left-handed and positioned  $90^\circ$  from the standard, and the  $\chi$  circle is also left-handed. There is no  $\Phi$  Eulerian angle adjustment. Selected were 13 ( $\Omega, \chi$ ) pairs of Eulerian angular settings to obtain 52 ( $13 \times 4$ ) independent time-of-flight neutron diffraction profiles, with a reasonable spread of sample orientation angles. Time-of-flight neutron diffraction profiles were collected for 4 h for all 13 settings.

### D. Monoclinic structural refinement with harmonics description

The structural refinements of high-resolution fixed-wavelength neutron powder diffraction data for the monoclinic phase at 20, 170, 220, 270, and 300 K were conducted using General Structure Analysis System (GSAS) (Larson and Von Dreele, 2000) with the generalized spherical-harmonics description [see Von Dreele (1997), Sitepu *et al.* (2002c, 2005), and references therein]. The initial monoclinic structure parameters were taken from the single-crystal

X-ray diffraction data of  $\text{Ti}_{50.80}\text{Ni}_{49.20}$  shape memory alloy (Kudoh *et al.*, 1985). Neutron scattering lengths at  $-3.44 \times 10^{-15}$  m and  $10.30 \times 10^{-15}$  m for Ti and Ni, respectively, were used. The scale factor, background function parameters (high order polynomials), profile parameters  $U$ ,  $V$ ,  $W$ , asymmetry coefficient, lattice parameters, atomic coordinates, mean square displacement factors, and site occupancies were varied in the refinement. After the refinement converged, harmonic coefficients,  $C_l^{mn}$  [see Eq. (3) of Sitepu *et al.* (2005)] were added to the refinement. The sample texture symmetry was chosen to be cylindrical, and a maximum of eight harmonic orders were selected (preliminary calculations with ten orders gave the same results).

### E. Texture determination of monoclinic time-of-flight neutron diffraction patterns

Fifty-two time-of-flight neutron diffraction patterns for the monoclinic crystal structure of  $\text{Ti}_{49.86}\text{Ni}_{50.14}$ , were refined simultaneously, using the multiple-data-set capabilities of the Rietveld refinement program GSAS with the generalized spherical-harmonics description. One single set of structural parameters for the monoclinic phase with space group  $P112_1/m$  (No. 11) and a generalized spherical-harmonics texture model up to eight orders were refined to fit the 52 patterns simultaneously. The texture coefficients  $C_l^{mn}$  were constrained to describe a texture of cylindrical sample symmetry. A part of the diffraction pattern where  $d$  spacings are greater than  $0.8 \text{ \AA}$  was used in the refinement. Approximately 400 reflections from the monoclinic phase of the Ni-rich  $\text{Ti}_{49.86}\text{Ni}_{50.14}$  alloy are contained within the range of  $d$  spacings greater than  $0.8 \text{ \AA}$ , and the entire suite of the time-of-flight neutron texture data consisted of approximately 70,000 data points. The data were corrected for absorption (Volz *et al.*, 2006), and three initial sample orientation angles were refined. For each diffraction pattern, one profile parameter and four background parameters were adjusted. The refinement strategy was similar to that described by Von Dreele (1997), Sitepu (2002), Sitepu *et al.* (2002b), and Sitepu *et al.* (2005). After the refinement converged, the first six [(010), (011), (100), (1 $\bar{1}$ 1), (101), and (110)] monoclinic pole-figures were calculated (designated measured pole-figures).

## III. RESULTS AND DISCUSSION

Figure 1(a) shows that there is one distinct differential scanning calorimeter peak on cooling (cubic to monoclinic martensitic phase transformation), and one peak on heating (monoclinic to cubic phase transformation). When this alloy is investigated at 300 K, it consists of a mixture of two phases (the cubic and the monoclinic phases) when 300 K was reached by either cooling from high temperatures, and pure monoclinic phase when 300 K was reached by heating from low temperatures. Figure 1(b) shows neutron powder diffraction patterns of the monoclinic phase at 20, 170, 220, 270, and 300 K, which are consistent with the differential scanning calorimeter results on heating. The quality of the Rietveld fits with generalized spherical-harmonics description for texture corrections at 20 and 300 K are given in Figures 2(a) and 2(b). Table I shows the refined atomic pa-

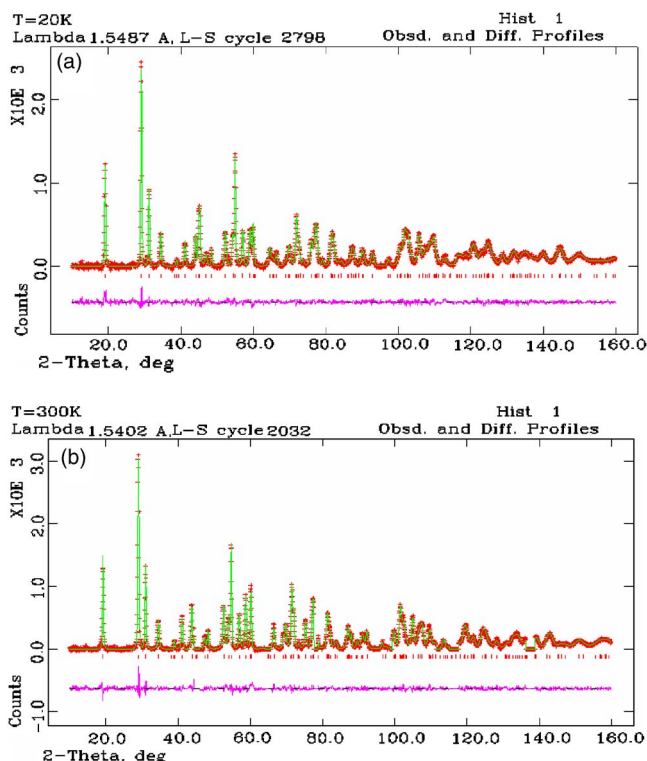


Figure 2. (Color online) The agreement between measured and calculated neutron powder diffraction patterns for the monoclinic phase in Ni-rich  $\text{Ti}_{49.86}\text{Ni}_{50.14}$  alloy at (a) 20 K and (b) 300 K on heating following Rietveld refinement with the generalized spherical-harmonics description for preferred orientation correction.

rameters for high-resolution neutron powder diffraction data sets of the monoclinic phase. Figure 3 shows the variation of temperature versus the  $\beta$  angle of the monoclinic phase. Figure 4 shows the calculated pole-figures derived from the orientation distribution function with the Williams-Imhof-Matthies-Vinel (WIMV) analysis [see Wenk *et al.* (2003) and references therein]. Table II depicts the texture comparison between the minimum and maximum values of pole-figures and orientation distribution function of the monoclinic phase in the Ni-rich  $\text{Ti}_{49.86}\text{Ni}_{50.14}$  alloy at 300 K.

### A. In situ structural refinement of monoclinic with neutron powder diffraction data

A single-crystal X-ray structure analysis by Kudoh *et al.* (1985) revealed that the  $\text{Ti}_{50.8}\text{Ni}_{49.2}$  alloy is monoclinic (martensitic, B19 phase) with unit cell parameters  $a = 2.898(1) \text{ \AA}$ ,  $b = 4.108(2) \text{ \AA}$ ,  $c = 4.646(3) \text{ \AA}$ ,  $\beta = 97.78(1)^\circ$ , and space group  $P112_1/m$  (No. 11). Their results agreed well with those reported by Michal and Sinclair (1981), but the quality of single-crystal X-ray diffraction data with 377 observed reflections reported by Kudoh *et al.* (1985) were superior to those of the single-crystal electron diffraction data with 22 observed reflections investigated by Michal and Sinclair (1981). Kudoh *et al.* (1985) reported that the Wyckoff positions occupied  $2e$  (0.5824, 0.2836, 0.2500) for Ti atoms and  $2e$  (0.0372, 0.1752, 0.7500) for Ni atoms.

The refined atomic parameters determined from Rietveld refinement for all neutron diffraction data sets of monoclinic phase at 20, 170, 220, 270, and 300 K are given in Table I.

TABLE I. Refined crystal structure parameters for the monoclinic phase in the high-resolution neutron powder diffraction data of Ni<sub>50.14</sub>Ti<sub>49.86</sub> alloy at 20, 120, 220, 270, and 300 K on heating. The space group used was  $P112_1/m$  (No. 11). Standard deviations in parentheses refer to the last digit. Wyckoff coordinates are  $2(e)=x, y, \frac{1}{4}$ , and  $2(e)=\bar{x}, \bar{y}, \frac{3}{4}$ . GOFI and  $U_{\text{iso}}$  are goodness-of-fit index and isotropic temperature factor, respectively;  $R_p$ ,  $R_{\text{wp}}$ , and  $R(F)^2$  are crystallographic  $R$  factors (figures-of-merit) and  $\chi^2$  and  $J$  are goodness-of-fit index and texture index, respectively. The values in the parenthesis (second lines) in the column for 300 K are the refined crystal structure parameters for a simultaneous refinement using 52 time-of-flight monoclinic neutron diffraction patterns with texture.

Refined parameters	Kudoh <i>et al.</i> (1985) (Single-crystal)	Atomic parameters				
		This study (polycrystalline sample)				
		20 K	170 K	220 K	270 K	300 K
$a$ (Å)	2.898(1)	2.89955(17)	2.88(4)	2.89(9)	2.89291(16)	2.89434(17) [2.89281(7)]
$b$ (Å)	4.108(2)	4.12865(18)	4.11(6)	4.12(13)	4.12181(16)	4.12672(18) [4.12628(1)]
$c$ (Å)	4.646(3)	4.69279(25)	4.65(7)	4.66(14)	4.64400(22)	4.63680(23) [4.63438(3)]
$\beta$ (°)	97.78(4)	97.9296(35)	97.679(4)	97.499(4)	97.3563(35)	97.1647(34) [97.1193(2)]
$V$ (Å <sup>3</sup> )	54.79(4)	55.64(1)	54.59(9)	55.08(6)	54.92(1)	54.95(1) [54.99(2)]
$x$	0.5824(5)	0.5933(9)	Ti( $x, y, \frac{1}{4}$ ) 0.5894(9)	0.5858(17)	0.5842(13)	0.5773(14) [0.5711(3)]
$y$	0.2836(3)	0.2857(5)	0.2850(6)	0.2823(11)	0.2881(10)	0.2841(9) [0.2780(2)]
$U_{\text{iso}}$ (Å) <sup>2</sup>	0.0107	0.018(8)	0.006(30)	0.001(1)	0.008(1)	0.009(1) [0.008(2)]
$x$	0.0372(4)	0.0389(4)	Ni( $\bar{x}, \bar{y}, \frac{3}{4}$ ) 0.0371(4)	0.0374(6)	0.0349(5)	0.0332(6) [0.0318(2)]
$y$	0.1752(2)	0.1752(2)	0.17474(25)	0.1752(4)	0.1782(4)	0.17791(34) [0.17560(1)]
$U_{\text{iso}}$ (Å) <sup>2</sup>	0.0126	0.018(28)	0.006(30)	0.004(1)	0.007(1)	0.007(1) [0.017(1)]
Figures-of-merit and GOFI						
$R_p$	4.5	3.02	3.03	2.93	3.10	3.14 [3.84]
$R_{\text{wp}}$	5.7	3.60	3.61	3.50	3.73	3.78 [5.83]
$R(F)^2$	N/A	2.14	2.01	1.53	3.49	3.04 [5.87]
$\chi^2$	N/A	1.03	1.04	1.00	1.36	1.39 [1.72]
$J$	N/A	1.32	1.27	1.38	1.49	1.43 [1.12]

The values in parentheses are estimated standard deviations. The refined atomic parameters for neutron data sets agree reasonably well with the single-crystal X-ray diffraction data reported by Kudoh *et al.* (1985). Figure 3 depicts the relationship between temperature and the  $\beta$  angle of the monoclinic phase, which indicates the value decreases with increasing temperature.

The quality of the measured high-resolution neutron powder diffraction data of the monoclinic phase in the Ni-rich Ti<sub>49.86</sub>Ni<sub>50.14</sub> alloy is shown in Figure 1(b). Figures 2(a) and 2(b) show the refinement results for the monoclinic phase measured at 20 and 300 K, respectively. The agreements are reasonably well between the measured and calculated diffraction patterns using multiple-data-set capabilities of the Rietveld refinement program GSAS with the generalized spherical-harmonics description for texture. The observed data are indicated by plus signs, and the calculated

profile is the continuous line. Vertical lines below the profiles represent the positions of all monoclinic possible Bragg reflections. The lower plot is the differences between the measured and calculated patterns on the same scale as the measured and calculated patterns. The figure-of-merit ranges from 3.50% to 3.78% for  $R_{\text{WP}}$  and 1.53% to 3.49% for  $R(F)^2$ . The values of texture index [see Eq. (4) of Sitepu *et al.* (2005)] range from 1.27 to 1.49, indicating that the polycrystalline alloy is a non-randomly orientated sample (with a moderate texture). It should be noted that the texture index is unity for an ideal randomly oriented powder specimen. The goodness-of-fit index ( $\chi^2$ ) values range from 1.1 to 1.5.

## B. *In situ* simultaneous refinement of 52 time-of-flight neutron diffraction patterns with texture

The GSAS Rietveld program with generalized spherical-

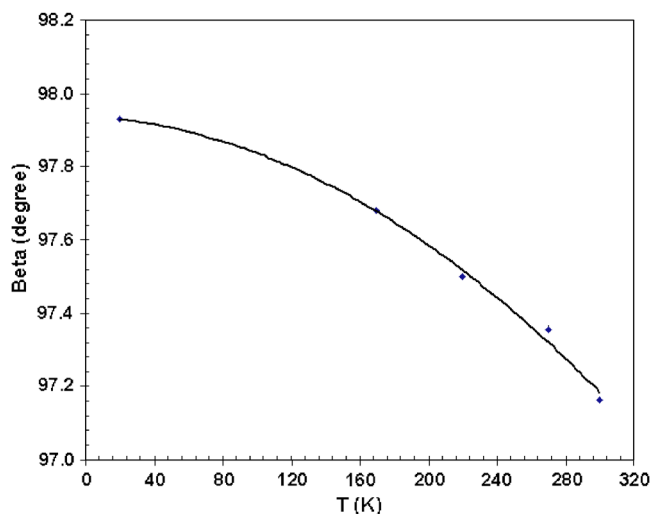


Figure 3. Plot of temperature versus the  $\beta$  angle of the monoclinic phase in  $\text{Ti}_{49.86}\text{Ni}_{50.14}$  shape memory alloy. Error bars are smaller than the symbols.

harmonics description (Von Dreele, 1997) and MAUD program with the WIMV method (Lutterotti *et al.*, 1997) offer the possibility for texture analysis of this low-crystal-symmetry material with many overlapping peaks. However, the harmonic expansion degree in the present GSAS version for texture analysis is limited by the finite number of measured data points over the pole-figure space, and also by the presence of possible artifacts in the orientation distribution function, particularly in cases of low-crystal symmetry. To overcome this problem, MAUD uses the WIMV method (Matthies *et al.*, 1988; 1997) to determine the best orientation distribution function reproducing the pole-figure texture values by maximizing the highest possible minimum value, which must be greater than zero, maximizing the texture sharpness, and assuming some properties of what is in essence the odd-order harmonic terms that cannot be determined from a diffraction experiment.

The GSAS Rietveld program was used to determine the texture of the alloy. The generalized spherical-harmonics is generated using selection rules depending on the crystal symmetry of the phase under investigation (Bunge 1982; Popa, 1992; Von Dreele, 1997). The multiple-dataset capabilities of the Rietveld refinement program GSAS was used successfully to extract the texture description directly from a

simultaneous refinement of 52 time-of-flight neutron diffraction patterns taken from the Ni-rich  $\text{Ti}_{49.86}\text{Ni}_{50.14}$  alloy held in 13 orientations in the diffractometer. This procedure is able to determine the texture of the monoclinic phase [see Figure 1(a)]. The results reveal that the refined crystal structure parameters agree reasonably well with the single-crystal X-ray diffraction data reported by Kudoh *et al.* (1985) (see Table I). At convergence, the figures-of-merit values range from 3.84% to 7.23% for  $R_p$ , 5.83% to 9.73% for  $R_{WP}$ , and 5.87% to 7.82% for  $R(F^2)$  with  $N_{\text{obs}}$  of 150, and the goodness-of-fit index ( $\chi^2$ ) is 1.72 for 415 variables. The measured (010), (011), (100), ( $\bar{1}\bar{1}$ 1), (101), and (110) monoclinic pole-figures derived from Rietveld refinement with generalized spherical-harmonics description were then subjected to a WIMV analysis to obtain a completed orientation distribution function [see Wenk *et al.* (2003) and references therein]. The orientation distribution functions from the WIMV analysis were used to recalculate the six pole-figures for comparison with the original set computed from the refined values of harmonic coefficients (see Figure 4); the texture goodness-of-fit index  $RP_0$  from this comparison are also listed in Table II. The orientation distribution functions produced by WIMV analysis of the six pole-figures agree with the pole-figures generated from GSAS Rietveld refinement with generalized spherical-harmonics description. The minimum ( $P_{\text{min}}$ ) and maximum ( $P_{\text{max}}$ ) pole-figure values are very similar; the maximum difference is no more than 0.35 multiple-of-random distributions in any one of the six pole-figures shown in Figure 4 and Table II. The orientation distribution function results show that less than 23% of the  $\text{Ti}_{49.86}\text{Ni}_{50.14}$  alloy was randomly oriented. Although individually measured pole-figures using a texture goniometer with a Eulerian cradle are subject to random measurement errors (making them not so self-consistent), the pole-figures obtained from simultaneous refinement of 52 neutron time-of-flight diffraction data with generalized spherical-harmonics description are completely self-consistent because they are generated from the harmonic coefficients (Von Dreele, 1997).

#### IV. SUMMARY AND CONCLUSION

The phase transformation temperature of the Ni-rich  $\text{Ti}_{49.86}\text{Ni}_{50.14}$  shape memory alloy was obtained using a dif-

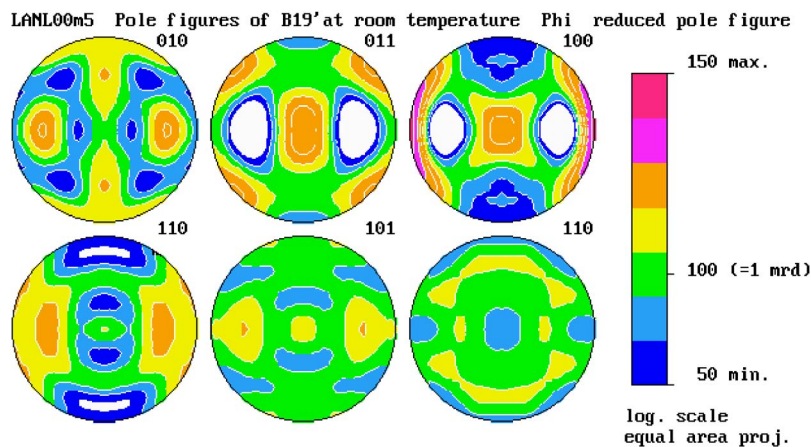


Figure 4. (Color online) Recalculated pole-figures of the monoclinic phase derived from orientation distribution function with WIMV. The  $\text{Ti}_{49.86}\text{Ni}_{50.14}$  sample rod axis is horizontal with respect to these pole-figures. As indicated in the text, prior to neutron texture data collection at room temperature, this alloy was kept in liquid nitrogen for 15 min so that it was in the monoclinic state after it warmed up to 300 K [see Arrow 5 in Figure 1(b), and a Rietveld fit in Figure 2(b)].

TABLE II. Texture comparison, minimum ( $P_{\min}$ ) and maximum ( $P_{\max}$ ) values of pole-figures, and orientation distribution function (ODF) of monoclinic phase in  $\text{Ni}_{50.14}\text{Ti}_{49.86}$  alloy at 300 K. Values of  $P_{\min}$  and  $P_{\max}$  are in multiples of random density (MRD). HIPD pole-figures are computed from the refined values of harmonic coefficients. Figures-of-merit  $RPO$  values are computed from pole figures generated from WIMV analysis; those in the ODF column represent averages over the six pole-figures.  $J$  is the texture index determined from Rietveld refinement with the generalized spherical harmonic description. If the texture is random, then  $J=1.00$ , otherwise  $J>1.00$ ; for single crystal  $J=\infty$ .

$hkl$	010	011	100	$\bar{1}\bar{1}$	101	110	ODF
HIPD, $J=1.117$							
$P_{\min}$	0.74	0.50	0.38	0.74	0.91	0.81	0.16
$P_{\max}$	1.34	1.39	1.66	1.23	1.19	1.10	2.26
$RPO$ (%)	1.08	2.28	1.71	1.35	1.04	1.08	1.42

ferential scanning calorimeter, and the *in situ* structural and texture of the monoclinic phase were determined successfully using the multiple-data-set capabilities of GSAS Rietveld refinement with generalized spherical-harmonics description and neutron powder diffraction data. The differential scanning calorimeter results revealed that there is one-step cubic to monoclinic martensitic phase transformation on cooling and one-step monoclinic to cubic transformation on heating. In addition, the start and finish transformation temperatures are 301 and 278 K, respectively, for the monoclinic phase on cooling, and 321 and 346 K, respectively, for cubic on heating. The measured neutron diffraction patterns of the monoclinic phase at 20, 170, 220, 270, and 300 K using the BT-1 high-resolution fixed-wavelength 32-detector powder diffractometer are consistent with the differential scanning calorimeter heating curve. The refined atomic parameters derived from Rietveld refinement with generalized spherical-harmonics description for all neutron diffraction data sets of this low-crystal-symmetry material agree satisfactorily with the monoclinic single-crystal X-ray diffraction data. Moreover, the multiple-data-set capabilities of the Rietveld refinement program GSAS with generalized spherical-harmonics description was successfully used to extract the texture description directly from a simultaneous refinement of 52 time-of-flight neutron diffraction patterns taken from the monoclinic structure in the polycrystalline  $\text{Ti}_{49.86}\text{Ni}_{50.14}$  sample held in 13 orientations in the diffractometer at room temperature. Finally, the maximum orientation distribution function is 2.26 multiple-of-random density, showing that this alloy consisted of 23% randomly oriented powders.

## ACKNOWLEDGMENTS

The author thanks J. K. Stalick of the NIST Center for Neutron Research and R. B. Von Dreele of Argonne National Laboratory for their invaluable contributions to the manuscript. The author acknowledges the support of the NIST and U.S. Department of Commerce in providing the neutron research facilities used in this work. The work also benefited from the use of the LANSCE, which is funded by the Basic Energy Sciences, Office of Science, U.S. Department of Energy. The author also acknowledges COMPRES under NSF Cooperative Agreement No. EAR 01-35554 for financial support.

Bunge, H.-J. (1982). *Texture Analysis in Materials Science: Mathematical Methods* (P. R. Morris, Trans.) (Butterworth-Heinemann, London).  
 Kudoh, Y., Tokonami, M., Miyazaki, S., and Otsuka, K. (1985). "Crystal

Structure of the Martensite in  $\text{Ti}_{50.8}\text{Ni}_{49.2}$  Alloy Analyzed by the Single Crystal X-ray Diffraction Method," *Acta Metall.* **33**, 2049–2056.  
 Larson, A. C. and Von Dreele, R. B. (2000). *General Structure Analysis System (GSAS)* (Report LAUR 86-748). Los Alamos, New Mexico: Los Alamos National Laboratory.  
 Lutterotti, L., Matthies, S., Wenk, H.-R., Schultz, A. S., and Richardson, Jr., J. W. (1997). "Combined Texture and Structure Analysis of Deformed Limestone from Time-of-flight Neutron Diffraction Spectra," *J. Appl. Phys.* **81**, 594–600.  
 Matthies, S., Wenk, H.-R., and Vinel, G. W. (1988). "Some Basic Concepts of Texture Analysis and Comparison of Three Methods to Calculate Orientation Distributions from Pole Figures," *J. Appl. Crystallogr.* **21**, 285–304.  
 Matthies, S., Lutterotti, L., and Wenk, H.-R. (1997). "Advances in Texture Analysis from Diffraction Spectra," *J. Appl. Crystallogr.* **30**, 31–42.  
 Michal, G. M., and Sinclair, R. (1981). "The Structure of Ti-Ni Martensite," *Acta Crystallogr.* **37**, 1803–1807.  
 Otsuka, K., and Ren, X. (2005). "Physical Metallurgy of Ti-Ni-based Shape Memory Alloys," *Prog. Mater. Sci.* **50**, 511–678.  
 Popa, N. C. (1992). "Texture in Rietveld Refinement," *J. Appl. Crystallogr.* **25**, 611–616.  
 Sitepu, H. (2002). "Assessment of Preferred Orientation with Neutron Powder Diffraction Data," *J. Appl. Crystallogr.* **35**, 274–277.  
 Sitepu, H. (2003). "Use of Synchrotron Diffraction Data for Describing Crystal Structure and Crystallographic Phase Analysis of R-phase NiTi Shape Memory Alloy," *Textures Microstruct.* **35**, 185–195.  
 Sitepu, H. (2007). "Structural Refinement of Neutron Powder Diffraction Data of Two-stage Martensitic Phase Transformations in  $\text{Ti}_{50.75}\text{Ni}_{47.75}\text{Fe}_{1.50}$  Shape Memory Alloy," *Powder Diffr.* **22**, 209–318.  
 Sitepu, H., Schmahl, W. W., Allafi, J. K., Eggeler, G., Dlouhy, A., Toebbens, D. M., and Tovar, M. (2002a). "Neutron Diffraction Phase Analysis During Thermal Cycling of a Ni-rich NiTi Shape Memory Alloy Using the Rietveld Method," *Scr. Mater.* **46**, 543–548.  
 Sitepu, H., Schmahl, W. W., and Von Dreele, R. B. (2002b). "Use of the Generalized Spherical Harmonic Model for Describing Crystallographic Texture in Polycrystalline NiTi Shape-memory Alloy with Time-of-flight Neutron Powder Diffraction Data," *Appl. Phys. A* **74**, S1676–S1678.  
 Sitepu, H., Schmahl, W. W., and Stalick, J. K. (2002c). "Correction of Intensities for Preferred Orientation in Neutron-diffraction Data of NiTi Shape-memory Alloy Using the Generalized Spherical-harmonic Description," *Appl. Phys. A* **74**, S1719–S1721.  
 Sitepu, H., O'Connor, B. H., and Li, D. (2005). "Comparative Evaluation of the March and Generalized Spherical Harmonic Preferred Orientation Models Using X-ray Diffraction Data for Molybdenite and Calcite Powders," *J. Appl. Crystallogr.* **38**, 158–167.  
 Volz, H. M., Vogel, S. C., Necker, C. T., Roberts, J. A., Lawson, A. C., Williams, D. J., Daemen, L. L., Lutterotti, L., and Pehl, J. (2006). "Rietveld Texture Analysis by Neutron Diffraction of Highly Absorbing Materials," *Adv. X-Ray Anal.* **49**, 156–162.  
 Von Dreele, R. B. (1997). "Quantitative Texture Analysis by Rietveld Refinement," *J. Appl. Crystallogr.* **30**, 517–525.  
 Wang, F. E., Buehler, W. J., and Pickart, S. J. (1965). "Crystal Structure and a Unique "Martensitic" Transition of TiNi," *J. Appl. Phys.* **36**, 3232–3239.  
 Wenk, H.-R., Lutterotti, L., and Vogel, S. (2003). "Texture Analysis With the New HIPPO TOF Diffractometer," *Nucl. Instrum. Methods Phys. Res. A* **515**, 575–588.